

UCSF

UC San Francisco Previously Published Works

Title

Immunosuppression With FTY720 Reverses Cardiac Dysfunction in Hypomorphic ApoE Mice Deficient in SR-BI Expression That Survive Myocardial Infarction Caused by Coronary Atherosclerosis

Permalink

<https://escholarship.org/uc/item/0s58w565>

Journal

Journal of Cardiovascular Pharmacology, 67(1)

ISSN

0160-2446

Authors

Luk, Fu Sang
Kim, Roy Y
Li, Kang
et al.

Publication Date

2016

DOI

10.1097/fjc.0000000000000312

Peer reviewed



Published in final edited form as:

J Cardiovasc Pharmacol. 2016 January ; 67(1): 47–56. doi:10.1097/FJC.0000000000000312.

Immunosuppression with FTY720 Reverses Cardiac Dysfunction in Hypomorphic ApoE Mice Deficient in SR-BI Expression that Survive:

Myocardial Infarction Caused by Coronary Atherosclerosis

Fu Sang Luk^{1,*}, Roy Y. Kim^{1,*}, Kang Li¹, Daniel Ching¹, David K. Wong¹, Sunil K. Joshi², Isabella Imhof², Norman Honbo², Holly Hoover², Bo-Qing Zhu², David H. Lovett², Joel S. Karliner², and Robert L. Raffai¹

¹Department of Surgery, San Francisco VA Medical Center/University of California, San Francisco

²Department of Medicine, San Francisco VA Medical Center/University of California, San Francisco

Abstract

Aims—We recently reported that immunosuppression with FTY720 improves cardiac function and extends longevity in Hypomorphic ApoE mice deficient in scavenger receptor Type-BI expression, also known as the HypoE/*SR-BI*^{-/-} mouse model of diet-induced coronary atherosclerosis and myocardial infarction (MI). In this study we tested the impact of FTY720 on cardiac dysfunction in HypoE/*SR-BI*^{-/-} mice that survive MI and subsequently develop chronic heart failure.

Methods/Results—HypoE/*SR-BI*^{-/-} mice were bred to Mx1-Cre transgenic mice and offspring were fed a high fat diet (HFD) for 3.5 weeks to provoke hyperlipidemia, coronary atherosclerosis and recurrent MIs. In contrast to our previous study, hyperlipidemia was rapidly reversed by inducible Cre-mediated gene repair of the HypoE allele and switching mice to a normal chow diet. Mice that survived the period of HFD were subsequently given oral FTY720 in drinking water or not, and left ventricular (LV) function was monitored using serial echocardiography for up to 15 weeks. In untreated mice, LV performance progressively deteriorated. Although FTY720 treatment did not initially prevent a decline of heart function among mice six weeks after Cre-mediated gene repair, it almost completely restored normal LV function in these mice by 15 weeks. Reversal of heart failure did not result from reduced atherosclerosis as the burden of aortic and coronary atherosclerosis actually increased to similar levels in both groups of mice. Rather, FTY720 caused systemic immunosuppression as assessed by reduced numbers of circulating T and B lymphocytes. In contrast, FTY720 did not enhance the loss of T cells or macrophages that accumulated in the heart during the HFD feeding period, but it did enhance the loss of B cells soon after plasma lipid lowering. Moreover, FTY720 potentially reduced the expression of matrix metalloproteinase-2 and genes involved in innate immunity-associated inflammation in the heart.

Correspondence to Robert L. Raffai, Ph.D., Department of Surgery, University of California, San Francisco and San Francisco VA Medical Center, 4150 Clement Street, San Francisco, CA 94121, Telephone: (415) 221-4810 ext. 2541, robert.raffai@ucsf.edu.

*These authors contributed equally

Conclusions—Our data demonstrate that immunosuppression with FTY720 prevents post-infarction myocardial remodeling and chronic heart failure.

Keywords

FTY720; S1P; ApoE; Coronary Atherosclerosis; Heart Failure; Cardioprotection; Immunosuppression

INTRODUCTION

Hyperlipidemia leading to occlusive coronary artery disease is a principal cause of myocardial infarction (MI). Once established, the infarct scar results in the dysfunctional remodeling of the adjacent and ultimately of the remote left ventricular myocardium.¹ The major clinical consequences of this remodeling process are progressive ventricular dysfunction and congestive heart failure (CHF). The pharmacologic treatment of heart failure has been static for many years and primarily consists of diuretics, β -blockers and suppression of angiotensin II activity with converting enzyme inhibitors or receptor blockade. Immunotherapy of post-infarction chronic heart failure has failed to gain traction among clinicians, largely because of adverse responses including ventricular rupture.² More recently a deeper understanding of the complex immune response that accompanies MI has led to the re-exploration of such therapy.^{3–5} A number of studies have recently demonstrated the impact of MI on subsequent leukocyte recruitment to the heart.⁶ Leukocytes of both myeloid and lymphoid origin have been shown to contribute not only to healing of the ischemic myocardial tissue but also to cardiac inflammation, ventricular remodeling and chronic heart failure.⁷

Sphingosine is a ubiquitous component of cell membranes and its phosphorylation by two related kinases yields the product sphingosine-1-phosphate (S1P).⁸ While initially studied within the context of cellular immunity, it has more recently become apparent that S1P is also a cardioprotective molecule. S1P plays a role in the control of cell migration, including lymphocyte trafficking,⁹ ischemia/reperfusion injury, cardiac muscle hypertrophy, endothelial function and wound healing.⁸ Analogues of S1P that regulate immune function have been developed and one of these, FTY720, has been approved by the FDA for the treatment of multiple sclerosis.¹⁰

As a consequence of its broad effects on the immune system, FTY720 has attracted attention for the treatment of atherosclerosis and cardiac injury.^{11–15} Several reports have indicated that FTY720 can suppress the onset and progression of atherosclerosis in mouse models of spontaneous and diet-induced atherosclerosis.^{16, 17} We recently reported that FTY720 prolongs survival in a mouse model of diet-induced coronary atherosclerosis and MI.¹⁸ These mice, referred to here as HypoE/*SR-BI*^{-/-} mice, display moderately elevated plasma HDL and can live a normal lifespan when fed a normal chow diet. On a high fat diet these mice rapidly develop marked hyperlipidemia, extensive occlusive coronary atherosclerosis and die within 4–7 weeks from recurrent MI and ischemic heart failure.^{18, 19} Our recent studies of these mice revealed that immunosuppression with FTY720 preserves left ventricular function and profoundly improves the survival of HypoE/*SR-BI*^{-/-} mice fed a

high fat diet.¹⁸ Remarkably, this effect did not originate from reduced coronary atherosclerosis, but rather from reduced systemic and cardiac inflammation.¹⁸

In the present study we sought to explore the impact of oral FTY720 on cardiac dysfunction in HypoE/*SR-BI*^{-/-} mice that survived recurrent MIs and ischemic cardiac injury caused by a 3.5-week period of HFD. To maximize the survival of HypoE/*SR-BI*^{-/-} mice fed a HFD we bred them to Mx1-Cre mice that in contrast to our prior study allows rapid and sustained restoration of normal apoE levels in plasma. Our recent studies of HypoE Mx1-Cre mice have shown that reducing hyperlipidemia in this manner can promote atherosclerosis regression and lesion stabilization in the aortic root.^{20, 21} Whether repair of the HypoE allele and use of FTY720 could promote coronary atherosclerosis regression in 3.5 week HFD-fed HypoE/*SR-BI*^{-/-} Mx1-Cre mice was also explored in this study.

METHODS

This study was conducted in accordance with the guide for the Care and Use of Laboratory Animals (National Academic Press, Washington, DC, 1996). All procedures were approved by the Animal Care Subcommittee of the San Francisco VA Medical Center and conform to NIH Guidelines.

Animal Model and Diet

As noted above in this study we made use of a mouse model of diet-induced coronary atherosclerosis that was created by breeding our previously reported hypomorphic apoE mice also known as “HypoE” mice that carry the ApoE61^{h/h} allele²² to mice deficient in SR-BI receptors referred to as HypoE/*SR-BI*^{-/-} mice, also termed here as HypoE/*SR-BI*^{-/-} mice.^{18, 19} We built upon our model by breeding HypoE/*SR-BI*^{-/-} mice to Mx1-Cre mice that we previously showed can cause the rapid repair of the HypoE allele resulting in restored normal apoE expression levels, normalization of hyperlipidemia and atherosclerosis regression in the aorta.^{20, 21} When HypoE/*SR-BI*^{-/-} Mx1-Cre mice were 3 months old, they were fed a high-fat diet (HFD) for 3.5 weeks which was then switched to a chow diet (2916; Harlan Taklad, Madison, WI), and induced to express normal apoE levels by two daily injections of 200 µg of polyinosinic:polycytidylic acid (pI-pC) in 1 ml of saline in the peritoneum. The HFD consisted of 16% fat and 1.25% cholesterol (D12336; Research Diets, Inc., New Brunswick, NJ). The timing of the switch was based on our prior experience which indicated that mice began to die of MI and heart failure at this time.¹⁸ FTY720 at a dose of 0.05 mg/kg/d was placed in the drinking water as previously described.¹⁸ Feeding of FTY720 was begun at 3.5 weeks post HFD and pI-pC induction and continued until mice were removed from the study 6–15 weeks later for biochemical and histologic analysis. All mice were maintained with a 12-hour light/12 hour dark cycle in the San Francisco VA Medical Center animal research facility.

Echocardiography

Transthoracic echocardiography was performed with a commercially available system (Acuson Sequoia c256, Acuson, Siemens) using a 15-MHz linear array transducer as previously described in our laboratory.¹⁸ Conscious mice were inserted into a plastic cone

after the anterior chest was shaved and then maneuvered into a prone position. Warm ultrasound transmission gel was then used to fill the gap between the chest and the cone, so that two-dimensional imaging could be performed through the cone. Two-dimensional long-axis images of the left ventricle (LV) were recorded at the plane of the aortic and mitral valves where the LV cavity is largest and a short-axis image was obtained at the papillary muscle level. The sweep speed for recording M-mode images was 200mm/s using two-dimensional guidance. All measurements were made from digital images captured on cine loops at the time of study with the use of a specialized software package (Acuson Sequoia) by an observer blinded to the therapy received by the mice. The LV end-diastolic dimension (LVEDD), end-systolic dimension (LVESD), and fractional shortening (FS) were measured as previously described.¹⁸ LV end-diastolic and end-systolic volumes and ejection fraction were also measured as described.¹⁸

Plasma Lipid Measurements

Blood was collected from cohorts of HypoE/*SR-BI*^{-/-} Mx1-Cre mice after 3.5 weeks of HFD following a 4-hour fast. Subsequently blood samples were collected up to the time of sacrifice. Mice were anesthetized by isoflurane inhalation and plasma was obtained from blood drawn by retro-orbital puncture. Colorimetric assays were used to measure cholesterol in plasma according to the manufacturer's instructions (Cholesterol E, L-type TG M; Wako, VA) using a VersaMax microplate reader (Molecular Devices Corporation, Sunnyvale, CA).

Morphologic and Histologic Analyses

Tissue collection—HypoE/*SR-BI*^{-/-} Mx1-Cre mice fed the HFD for 3.5 weeks and treated with or without FTY720 were sacrificed either at 6 or 15 weeks after stopping of HFD. Mice were weighed and anesthetized with 2.5% tribromoethanol (Avertin). After thoracotomy, mice were perfused via heart puncture with 10ml ice-cold PBS containing RNase inhibitors (ProtectRNA™; Sigma, MO) for 1 min. Hearts were collected, weighed and cut in half. The basal portion was embedded in tissue freezing medium (OCT) that was flash frozen in an isopentane bath cooled with liquid nitrogen and the apical portion was flash frozen in liquid nitrogen for RNA or protein analysis.

Cryosectioning and Staining—Atherosclerosis and histology were assessed by obtaining simultaneous serial sections of the basal portion of the heart subdivided into 2 segments as previously described.¹⁸ Serial 10µm sections were collected on 5 different slides from each segment. Serial 10µm sections also were cut from the root of the aorta through the aortic sinuses encompassing a total length of 500–600 µm (3 sections per slide). Slides from each segment were used for immuno-staining or were stained with Oil Red O (ORO) or Picro Sirius Red counterstained with Fast Green.

Quantification of Occlusive Coronary Atherosclerosis—The extent and severity of coronary atherosclerosis was quantified in a blinded fashion by counting vessels in twelve or more heart sections per mouse stained with Picro Sirius Red to reveal collagen as previously described.¹⁸ Scoring the extent of occlusion in the coronary arteries was performed by visual inspection of the slides at a power of 100×. Vessels were defined as non-occluded (NO) with a 0–5% burden, partially occluded (PO) with a 5–50% burden, severely occluded (SO) with

a 50–95% burden, and completely occluded (CO) with a 95–100% burden. Calculating the average percent of obstructed vessels in each category provided an index of vessel occlusion.¹⁹

Quantification of Aortic Atherosclerosis—For morphologic analysis, sections of the aortic sinuses were stained with Oil Red O or Picro Sirius Red and counterstained with Fast-Green. The atherosclerotic burden in the aortic root was quantified in a blinded fashion using six sections per mouse as we previously described.^{18, 20, 23, 24} Metamorph software (Molecular Devices Inc., Sunnyvale, CA) was used to quantify the lesion area per cross section, which was then averaged to provide mean lesion area per mouse.

Flow Cytometry

Multicolor flow cytometry was performed using standard procedures. Peripheral blood was drawn and blocked with an anti-CD16/CD32 (2.4G2; UCSF Cell Culture Facility) for 10 min. Without washing, the cells were then incubated with pre-mixed combinations of antibodies. FITC-conjugated anti-B220, anti-Ly6C, and anti-CD4; PE-conjugated anti-CD3e, anti-Ly6G, and anti-CD44; PE-Cy7-conjugated anti-NK1.1 and anti-CD8; PerCP-Cy5.5-conjugated anti-CD11b; APC-conjugated anti-CD45 and anti-CD62L antibodies were all purchased from BD Biosciences. Data were acquired on an Accuri C6 Flow Cytometer using CFlow Plus software (BD Biosciences) and analyzed with FlowJo (TreeStar Inc.) as previously described.¹⁸

Quantitative Reverse Transcription Polymerase Chain Reaction (qRT-PCR)

Total RNA from mouse heart samples was isolated using an RNeasy Mini Kit (Qiagen Inc., Valencia, CA) according to the manufacturer's instructions. Isolated RNA was quantified and 1 μ g was used to synthesize cDNA using a Transcriptor First Strand cDNA Synthesis Kit (Roche Applied Bioscience Inc., Indianapolis, IN.). qRT-PCR was performed to quantify the expression of genes associated with select immune cells, pro-inflammatory cytokines, innate immunity markers, and MMP-2 isoforms using a LightCycler 480 SYBR Green I Master Kit (Roche Applied Bioscience Inc.) or TaqMan® Fast Advanced Master Mix (Life Technologies) Each biological sample was plated in triplicate in a 384 well PCR plate (Thermo Fisher, Waltham, MA). Taqman qPCR was performed using 40 cycles at 95°C for 15 seconds and 60°C for 1 minute and normalized to GAPDH. SYBR Green amplification reactions were performed using 40 cycles at 95°C for 15s; 58°C for 45s; and 72°C for 1 min and normalized to β -2-microglobulin. Melt curves were used to verify absence of primer dimers and other non-specific products in the amplification reactions. All reactions were performed on an Applied Biosystems 7900HT instrument. TaqMan® Assay IDs and SYBR Green I primer sequences are listed in Tables 1 and 2. Fold-change in mRNA expression was calculated by using the $\Delta\Delta$ CT method.

Statistical Analysis—All statistical analyses were performed using GraphPad Prism 5.0 (GraphPad Software). Data are expressed as the mean \pm SEM. Differences between experimental groups were analyzed for statistical significance by unpaired Student's t test or by 1-way ANOVA followed by Bonferroni test for the selected pairs. A *P* value of less than 0.05 was considered significant.

Results

Survival Data

As shown in Figure 1A, HypoE/*SR-BI*^{-/-} Mx1-Cre mice began to die just prior to the time when they were induced with pI-pC and switched from the HFD to a normal chow diet. This timing reproduced our prior mortality experience caused by diet-induced MI and acute heart failure.¹⁸ After less than a week following normalization of plasma lipid levels there was an initial loss of 40% of the mice after which there were no further deaths until much later when one mouse died (Figure 1A).

Effects of *ApoE* gene repair on plasma lipoprotein cholesterol levels and atherosclerosis

The data in Figure 1B demonstrate that pI-pC—induced ApoE gene repair and return to a chow diet resulted in rapid normalization of plasma cholesterol levels. Such abrupt and beneficial correction of hyperlipidemia likely contributed to the survival of a majority of the pI-pC—induced HypoE/*SR-BI*^{-/-} Mx1-Cre mice that were subjected to serial echocardiography as detailed below. The benefit of ApoE gene repair and plasma cholesterol normalization on atherosclerosis was explored in both the aortic root and coronary arteries. Contrary to our expectations and prior observations in the HypoE mouse model,^{20, 21} our current data provided no evidence of atherosclerosis regression in HypoE/*SR-BI*^{-/-} Mx1-Cre mice. These observations are also consistent with the report of Keul et al.²⁵ In contrast, we found evidence of continued atherosclerosis progression both in the aortic root and in the coronary bed (Figure 2 and 3). Moreover, we did not observe any benefit of FTY720 on altering the burden of atherosclerosis in either vascular bed.

Echocardiography: measurements of left ventricular function

Serial echocardiography revealed the expected decline in LV function and increase in volumes compared with baseline (Figure 4). These data are consistent with our prior report¹⁸ and also demonstrate that inducible Cre-mediated *ApoE* gene repair and rapid plasma cholesterol normalization in HypoE/*SR-BI*^{-/-} Mx1-Cre mice represent a new approach to generate a murine chronic heart failure model. After treatment with oral FTY720, serial echocardiography surprisingly revealed almost complete recovery of LV function and smaller LV volumes, particularly end systolic volumes. This occurred despite the absence of coronary atherosclerosis regression that actually became more obstructive over time as noted above (Figure 3). Conversely, control mice not treated with FTY720 displayed no recovery of LV performance, and showed persistent and progressive functional depression and increase in volumes, particularly end-systolic volume. Thus, in this mouse model, FTY720 can reverse depressed myocardial function and decrease ventricular volumes despite persistent coronary artery obstruction.

Leukocyte responses in the blood

In Figure 5 the blood leukocyte response after discontinuation of the high fat diet is shown. Feeding a normal chow diet did not dampen the progressive rise in T and B cells over the next 15 weeks in pI-pC—induced HypoE/*SR-BI*^{-/-} Mx1-Cre mice that did not receive FTY720, while the numbers of neutrophils and monocytes remained unchanged. These data

suggest that episodes of recurrent MI caused by HFD-driven occlusive coronary atherosclerosis result in a pronounced increase in circulating lymphocytes that are suppressed by FTY720. Such an effect was not observed among circulating myeloid cells, including neutrophils and monocytes which remained at constant levels. In addition there was no noticeable impact of FTY720 on these myeloid cells. In contrast, persistently elevated levels of circulating monocytes and neutrophils likely contributed to the observed continued progression of atherosclerosis in both the aortic root and coronary arteries among mice treated with FTY720 or sham, as suggested by Keul et al.¹⁶

Leukocyte responses in the heart

To explore the impact of immunosuppression by FTY720 on cardiac inflammation, we quantified markers for a panel of leukocyte mRNAs in heart specimens harvested from mice after 3.5 weeks of HFD, 6 and 15 weeks after plasma lipid reduction with and without FTY720 treatment. As shown in Figure 6, a 3.5 week period of HFD caused a marked increase in CD45⁺ leukocytes in the heart including F4/80⁺ macrophages along with CD4⁺ T cells and B220⁺ B cells, likely as a direct consequence of recurrent MI. Such marked cardiac inflammation was resolved after fifteen weeks of plasma lipid reduction as assessed by a substantial loss of all these leukocytes from the heart of mice examined at this time point. Interestingly, although our data show that FTY720 did not enhance loss of CD4⁺ T cells and F4/80⁺ macrophages in cardiac tissue of mice that survived 15 weeks post HFD, it did lead to a rapid loss of B220⁺ B cells 6 weeks after plasma lipid reduction (Figure 6). These findings suggest that the beneficial effect of FTY720 on promoting recovery of LV performance among mice that survive HFD-induced MI may be dependent on a rapid loss of B cells but not of other cardiac leukocytes.

FTY720 suppresses cardiac matrix metalloproteinase-2, MMP-14 and innate immunity gene expression

Experimental and clinical studies have defined a pivotal role for the full length MMP-2 isoform (FL-MMP-2) in post-infarction ventricular remodeling.^{26–29} Recent studies from our laboratories have characterized an additional intracellular isoform of MMP-2 generated by oxidative stress-mediated activation of an alternate promoter located in the first intron of the MMP-2 gene.³⁰ This process generates an N-terminal truncated MMP-2 isoform (NTT-MMP-2) that is enzymatically active and localized to mitochondria. NTT-MMP-2 initiates a type I interferon-like response with expression of a defined group of primary innate immunity genes associated with inflammation and severe systolic failure.^{30–32} As detailed in Figure 7A, 3.5 weeks of a HFD induced a greater than 6-fold increase in the FL-MMP-2 transcript in the heart. FL-MMP-2 transcript abundance remained elevated over 5-fold six weeks following normalization of plasma lipids and the abundance of this transcript was reduced significantly by treatment with FTY720. While abundance of this FL-MMP-2 transcript remained modestly elevated at 15 weeks following lipid normalization, there was no significant further reduction by FTY720 at this time. As with the FL-MMP-2 transcript, there was a significant four-fold increase in NTT-MMP-2 transcript abundance after 3.5 weeks of high fat diet, which remained significantly elevated at 6 and 15 weeks following lipid normalization. Although there was a trend for a reduction in NTT-MMP-2 transcript

abundance with FTY720 treatment, it did not reach statistical significance in our cohort of mice (Figure 7B).

We also examined expression of MMP-9 and MMP-14 and determined the potential effects of FTY720 on these. As summarized in Figure 7, MMP-9 expression was significantly elevated following HFD and returned to baseline by 15 weeks. FTY720 did not suppress MMP-9 expression. MMP-14 levels were significantly elevated at 6 weeks but were suppressed by FTY720. MMP-14 levels returned to baseline by 15 weeks.

We next examined the transcript abundance of the pro-inflammatory cytokine interleukin 6 (IL-6), as well as three genes associated with a primary innate immune response including: Interferon Response Factor-7 (IRF-7), Interferon-Induced Protein with Tetratricopeptide Repeat 1 (IFIT1) and 2'-5' -oligoadenylate synthetase 1A (OAS1A) (Figure 8). While all transcripts were significantly elevated following 3.5 weeks of HFD, all manifested further highly significant elevations at 6 and 15 weeks following normalization of plasma lipids. FTY720 treatment suppressed transcription of IRF-7, OAS1A and IL-6, but did not affect the transcript abundance of IFIT1. Lastly, we measured levels of the B cell-specific cytokine chemokine (C-C motif) ligand 7 (CCL7) that has recently been associated with enhanced cardiac inflammation and CHF after MI in mice.⁵ As shown in Figure 8, CCL7 expression was profoundly upregulated following 3.5 weeks of HFD which correlates with increased numbers of cardiac B cells. Moreover, we also observed that its expression was profoundly reduced 6 weeks after FTY720 treatment that also led to a rapid loss of B cells. In summary, our findings demonstrate that FTY720 prevented pathological remodeling of the heart by reducing MMP-2 expression, and reducing a cytokine storm involving IL-6 and CCL7 as well as an excessive expression of immune genes including IRF-7 and OAS1A.

DISCUSSION

The combined contributions of immunity and inflammation to the pathogenesis of post-infarction CHF has been increasingly recognized.⁷ The relevance of such phenomena to human CHF is not clear as the rodent models used to explore this pathophysiology have relied primarily on the permanent left anterior descending ligation model of myocardial infarction injury. In contrast, human CHF often develops among individuals who survive recurrent episodes of MI caused by progressive occlusive coronary atherosclerosis driven primarily by hyperlipidemia. Therefore, to better approximate the causative factors of human CHF we generated a mouse model in which CHF could be induced through dietary-mediated manipulation of plasma lipid levels. To this end, we improved our existing mouse model of diet-induced coronary atherosclerosis and fatal MI known as HypoE/*SR-BI*^{-/-} mice that we refer to as HypoE/*SR-BI*^{-/-} mice in this study. By breeding HypoE/*SR-BI*^{-/-} mice to Mx1-Cre mice, we introduced a genetic switch to rapidly normalize plasma lipid levels through inducible Cre-mediated gene repair of the HypoE allele. Our prior studies of variant forms of HypoE Mx1-Cre mice revealed the utility of this system to investigate biological mechanisms of atherosclerosis regression and lesion stabilization.^{20, 21} But whether such as an approach could be used to successfully study the process of coronary atherosclerosis regression and CHF in HypoE/*SR-BI*^{-/-} Mx1-Cre mice was less predictable because of the pronounced phenotype of rapid sudden death from MI.

Our data demonstrate that a rapid and sustained reduction of plasma lipid levels after 3.5 weeks of HFD permits survival in 60% of all HypoE/*SR-BI*^{-/-} Mx1-Cre mice. Serial echocardiograms of these mice over the next 15 weeks subsequently demonstrated development of progressive LV dysfunction with markedly reduced ejection fractions and elevated end-systolic volumes. Our findings also show that treatment with the immunosuppressant FTY720 at the time of Cre-mediated gene repair and lipid normalization resulted in an almost complete recovery of LV systolic function. The restoration of left ventricular systolic function occurred despite continued atherosclerosis progression in the aortic root and coronary arteries.

The mechanisms responsible for the recovery from LV systolic dysfunction are not entirely clear, but our data strongly suggest that immune suppression is a key factor in the improvement of LV performance. Specifically, our data point to excessive IL-6 expression as a direct contributor to CHF in the setting of ischemic cardiac injury, and demonstrate the clinical benefit of reducing innate immune responses as a therapy to preserve and possibly restore heart function after MI. Specifically, our findings show the benefit of rapid elimination of cardiac B cells along with reduced CCL7 expression in preventing pathological remodeling and CHF. Such data support recent observations reporting a pathological role for B cells and B cell-derived CCL7 expression as a cause of enhanced cardiac inflammation and CHF that resulted from enhanced influx of circulating monocytes.⁵ Although reduced CCL7 expression following FTY720 treatment did not result in greater reduction of cardiac macrophages at the 6 week time point, we cannot exclude the possibility of an earlier loss of these myeloid cells after lipid lowering and FTY720 initiation. Future time-course studies will be required to address this issue.

Both MMP-2 isoforms are associated with decreased systolic function due to disruption of either sarcomeric integrity or excitation-associated calcium handling.^{28, 31} Full length MMP-2 transcription can be driven by IL-6 via the STAT signaling cascade and it is most probable that the decreases in FL-MMP-2 following FTY720 treatment are the result of inhibition of IL6 synthesis.^{33, 34} The NTT-MMP-2 isoform lacks a STAT binding site in the intronic promoter, which is the most probable explanation for the absence of a FTY720 inhibitory effect on this isoform. Thus, the improvement in ventricular function may be ascribed to FTY720 suppression of FL-MMP-2 isoform expression.

During post-infarction remodeling MMP-9 is primarily expressed by infiltrating inflammatory cells, while MMP-14 is expressed by both cardiac fibroblasts and cardiomyocytes.^{35, 36} The promoter regions of MMP-9 and MMP-14 are structurally very distinct and likely that this is the explanation for the variable responses to FTY720.^{37, 38} The suppression of MMP-14 by FTY720 is a likely contributor to the improved ventricular function observed in treated mice. MMP-14 acts at multiple levels in post-infarction ventricular remodeling, including alterations in cardiac extracellular matrix and activation of latent transforming growth factor-beta-1.³⁶ Further, MMP-14 is a key activator of latent MMP-2 which may further contribute to systolic failure.³⁹

Our findings partially reproduce and extend earlier studies conducted in ApoE null mice subjected to LAD ligation as a model of MI and CHF.⁴⁰ Similar to results of that study, we

noted that recurrent MI led to pronounced atherosclerosis in the aorta. Our findings also show that coronary atherosclerosis worsens after MI. However, in pIpC-induced HypoE/SR-BI^{-/-} Mx1-Cre mice the continued progression of atherosclerosis after lipid lowering was not due to increased monocytophilia as levels of circulating monocytes and neutrophils remained similar to baseline values. Rather, a reason for persistent atherosclerosis and lack of atherosclerosis lesion regression and stabilization in this model could be due to the absence of the SR-BI receptor that participates in the removal of cellular cholesterol from lesional macrophages and to its disposal in the liver via HDL.⁴¹ Irrespective of the cause of continued atherosclerosis progression it did not cause fatal MI among the mice at the 15 week time point.

Notwithstanding the continued increase in the burden of coronary atherosclerosis, a large proportion of pIpC-induced mice survived up to the point of harvest that was 15 weeks after plasma lipid reduction. One possibility to explain survival among these mice is that the burden of occlusive coronary atherosclerosis did not reach a critical threshold level. Indeed, our prior studies of the model fed a HFD for a longer period of time resulted in far lower numbers of coronary arteries free of disease.¹⁹ A larger proportion of coronary arteries with no evidence of atherosclerosis suggests the formation of collateral vessels resulting in reduced cardiac ischemia that could explain survival in these mice.

In summary, the most noteworthy finding of our study is the observation that the immunosuppressant FTY720 can almost completely reverse cardiac dysfunction in HypoE/SR-BI^{-/-} Mx1-Cre mice. Our data suggest that a suppression of systemic adaptive immunity contributed to this recovery, as mice not treated with FTY720 developed progressively increased numbers of lymphocytes in the circulation. This effect was partially reproduced in the heart. Although mice treated with FTY720 did not display a more substantial reduction of T cells and macrophages in the heart after plasma lipid lowering, it did result in a more rapid loss of B cells and its associated chemokine CCL7 that has recently been shown to contribute to cardiac inflammation by enhancing the recruitment of monocytes into the infarcted heart.⁵ Also, FTY720 likely impacted the phenotypic behavior of leukocytes in the heart resulting in a marked suppression of MMP-2 expression that led to excessive ventricular remodeling in mice not treated with FTY720. In addition, FTY720 prevented a massive 100-fold increase the mRNA expression of IL-6 that is known to be cytotoxic to cardiomyocytes⁴² and also drives the expression of MMP-2.^{33, 34}

Ongoing studies are exploring the impact of FTY720 on altering the phenotype of cardiac immune cells and determining the impact that this can exert on reducing tissue inflammation and sparing LV function.

References

1. Dixon JA, Spinale FG. Myocardial remodeling: cellular and extracellular events and targets. *Annu Rev Physiol.* 2011; 73:47–68. [PubMed: 21314431]
2. Roberts R, DeMello V, Sobel BE. Deleterious effects of methylprednisolone in patients with myocardial infarction. *Circulation.* 1976 Mar; 53(3 Suppl):I204–I206. [PubMed: 1253361]

3. Frangogiannis NG. The immune system and the remodeling infarcted heart: cell biological insights and therapeutic opportunities. *J Cardiovasc Pharmacol.* 2014 Mar; 63(3):185–195. [PubMed: 24072174]
4. Frantz S, Nahrendorf M. Cardiac macrophages and their role in ischaemic heart disease. *Cardiovasc Res.* 2014 May 1; 102(2):240–248. [PubMed: 24501331]
5. Zouggari Y, Ait-Oufella H, Bonnin P, Simon T, Sage AP, Guerin C, Vilar J, Caligiuri G, Tsiantoulas D, Laurans L, Dumeau E, Kotti S, Bruneval P, Charo IF, Binder CJ, Danchin N, Tedgui A, Tedder TF, Silvestre JS, Mallat Z. B lymphocytes trigger monocyte mobilization and impair heart function after acute myocardial infarction. *Nat Med.* 2013 Oct; 19(10):1273–1280. [PubMed: 24037091]
6. Dutta P, Nahrendorf M. Monocytes in Myocardial Infarction. *Arterioscler Thromb Vasc Biol.* 2015 Mar 19.
7. Frieler RA, Mortensen RM. Immune cell and other noncardiomyocyte regulation of cardiac hypertrophy and remodeling. *Circulation.* 2015 Mar 17; 131(11):1019–1030. [PubMed: 25779542]
8. Karliner JS. Sphingosine kinase and sphingosine 1-phosphate in the heart: a decade of progress. *Biochim Biophys Acta.* 2013 Jan; 1831(1):203–212. [PubMed: 22735359]
9. Pappu R, Schwab SR, Cornelissen I, Pereira JP, Regard JB, Xu Y, Camerer E, Zheng YW, Huang Y, Cyster JG, Coughlin SR. Promotion of lymphocyte egress into blood and lymph by distinct sources of sphingosine-1-phosphate. *Science.* 2007 Apr 13; 316(5822):295–298. [PubMed: 17363629]
10. Brinkmann V. Sphingosine 1-phosphate receptors in health and disease: mechanistic insights from gene deletion studies and reverse pharmacology. *Pharmacol Ther.* 2007 Jul; 115(1):84–105. [PubMed: 17561264]
11. Jin ZQ, Zhang J, Huang Y, Hoover HE, Vessey DA, Karliner JS. A sphingosine kinase 1 mutation sensitizes the myocardium to ischemia/reperfusion injury. *Cardiovasc Res.* 2007 Oct 1; 76(1):41–50. [PubMed: 17610857]
12. Liu W, Zi M, Naumann R, Ulm S, Jin J, Taglieri DM, Prehar S, Gui J, Tsui H, Xiao RP, Neyses L, Solaro RJ, Ke Y, Cartwright EJ, Lei M, Wang X. Pak1 as a novel therapeutic target for antihypertrophic treatment in the heart. *Circulation.* 2011 Dec 13; 124(24):2702–2715. [PubMed: 22082674]
13. Liu W, Zi M, Tsui H, Chowdhury SK, Zeef L, Meng QJ, Travis M, Prehar S, Berry A, Hanley NA, Neyses L, Xiao RP, Oceandy D, Ke Y, Solaro RJ, Cartwright EJ, Lei M, Wang X. A novel immunomodulator, FTY-720 reverses existing cardiac hypertrophy and fibrosis from pressure overload by targeting NFAT (nuclear factor of activated T-cells) signaling and periostin. *Circ Heart Fail.* 2013 Jul; 6(4):833–844. [PubMed: 23753531]
14. Sattler K, Levkau B. Sphingosine-1-phosphate as a mediator of high-density lipoprotein effects in cardiovascular protection. *Cardiovasc Res.* 2009 May 1; 82(2):201–211. [PubMed: 19233866]
15. Vessey DA, Kelley M, Li L, Huang Y, Zhou HZ, Zhu BQ, Karliner JS. Role of sphingosine kinase activity in protection of heart against ischemia reperfusion injury. *Med Sci Monit.* 2006 Oct; 12(10):Br318–Br324. [PubMed: 17006394]
16. Keul P, Lucke S, von Wnuck Lipinski K, Bode C, Graler M, Heusch G, Levkau B. Sphingosine-1-phosphate receptor 3 promotes recruitment of monocyte/macrophages in inflammation and atherosclerosis. *Circ Res.* 2011 Feb 4; 108(3):314–323. [PubMed: 21164103]
17. Nofer JR, Bot M, Brodde M, Taylor PJ, Salm P, Brinkmann V, van Berkel T, Assmann G, Biessen EA. FTY720, a synthetic sphingosine 1 phosphate analogue, inhibits development of atherosclerosis in low-density lipoprotein receptor-deficient mice. *Circulation.* 2007 Jan 30; 115(4):501–508. [PubMed: 17242282]
18. Wang G, Kim RY, Imhof I, Honbo N, Luk FS, Li K, Kumar N, Zhu BQ, Eberle D, Ching D, Karliner JS, Raffai RL. The immunosuppressant FTY720 prolongs survival in a mouse model of diet-induced coronary atherosclerosis and myocardial infarction. *J Cardiovasc Pharmacol.* 2014 Feb; 63(2):132–143. [PubMed: 24508946]
19. Zhang S, Picard MH, Vasile E, Zhu Y, Raffai RL, Weisgraber KH, Krieger M. Diet-induced occlusive coronary atherosclerosis, myocardial infarction, cardiac dysfunction, and premature

- death in scavenger receptor class B type I-deficient, hypomorphic apolipoprotein ER61 mice. *Circulation*. 2005 Jun 28; 111(25):3457–3464. [PubMed: 15967843]
20. Eberle D, Luk FS, Kim RY, Olivas VR, Kumar N, Posada JM, Li K, Gaudreault N, Rapp JH, Raffai RL. Inducible ApoE gene repair in hypomorphic ApoE mice deficient in the low-density lipoprotein receptor promotes atheroma stabilization with a human-like lipoprotein profile. *Arterioscler Thromb Vasc Biol*. 2013 Aug; 33(8):1759–1767. [PubMed: 23788760]
 21. Raffai RL, Loeb SM, Weisgraber KH. Apolipoprotein E promotes the regression of atherosclerosis independently of lowering plasma cholesterol levels. *Arterioscler Thromb Vasc Biol*. 2005 Feb; 25(2):436–441. [PubMed: 15591220]
 22. Raffai RL, Weisgraber KH. Hypomorphic apolipoprotein E mice: a new model of conditional gene repair to examine apolipoprotein E-mediated metabolism. *J Biol Chem*. 2002 Mar 29; 277(13):11064–11068. [PubMed: 11792702]
 23. Eberle D, Kim RY, Luk FS, de Mochel NS, Gaudreault N, Olivas VR, Kumar N, Posada JM, Birkeland AC, Rapp JH, Raffai RL. Apolipoprotein E4 domain interaction accelerates diet-induced atherosclerosis in hypomorphic Arg-61 apoE mice. *Arterioscler Thromb Vasc Biol*. 2012 May; 32(5):1116–1123. [PubMed: 22441102]
 24. Gaudreault N, Kumar N, Posada JM, Stephens KB, Reyes de Mochel NS, Eberle D, Olivas VR, Kim RY, Harms MJ, Johnson S, Messina LM, Rapp JH, Raffai RL. ApoE suppresses atherosclerosis by reducing lipid accumulation in circulating monocytes and the expression of inflammatory molecules on monocytes and vascular endothelium. *Arterioscler Thromb Vasc Biol*. 2012 Feb; 32(2):264–272. [PubMed: 22053073]
 25. Keul P, Tolle M, Lucke S, von Wnuck Lipinski K, Heusch G, Schuchardt M, van der Giet M, Levkau B. The sphingosine-1-phosphate analogue FTY720 reduces atherosclerosis in apolipoprotein E-deficient mice. *Arterioscler Thromb Vasc Biol*. 2007 Mar; 27(3):607–613. [PubMed: 17158351]
 26. Alfonso-Jaume MA, Bergman MR, Mahimkar R, Cheng S, Jin ZQ, Karliner JS, Lovett DH. Cardiac ischemia-reperfusion injury induces matrix metalloproteinase-2 expression through the AP-1 components FosB and JunB. *Am J Physiol Heart Circ Physiol*. 2006 Oct; 291(4):H1838–H1846. [PubMed: 16699069]
 27. Bergman MR, Teerlink JR, Mahimkar R, Li L, Zhu BQ, Nguyen A, Dahi S, Karliner JS, Lovett DH. Cardiac matrix metalloproteinase-2 expression independently induces marked ventricular remodeling and systolic dysfunction. *Am J Physiol Heart Circ Physiol*. 2007 Apr; 292(4):H1847–H1860. [PubMed: 17158653]
 28. Wang GY, Bergman MR, Nguyen AP, Turcato S, Swigart PM, Rodrigo MC, Simpson PC, Karliner JS, Lovett DH, Baker AJ. Cardiac transgenic matrix metalloproteinase-2 expression directly induces impaired contractility. *Cardiovasc Res*. 2006 Feb 15; 69(3):688–696. [PubMed: 16183043]
 29. Zhou HZ, Ma X, Gray MO, Zhu BQ, Nguyen AP, Baker AJ, Simonis U, Cecchini G, Lovett DH, Karliner JS. Transgenic MMP-2 expression induces latent cardiac mitochondrial dysfunction. *Biochem Biophys Res Commun*. 2007 Jun 22; 358(1):189–195. [PubMed: 17475219]
 30. Lovett DH, Mahimkar R, Raffai RL, Cape L, Maklashina E, Cecchini G, Karliner JS. A novel intracellular isoform of matrix metalloproteinase-2 induced by oxidative stress activates innate immunity. *PLoS One*. 2012; 7(4):e34177. [PubMed: 22509276]
 31. Lovett DH, Chu C, Wang G, Ratcliffe MB, Baker AJ. A N-terminal truncated intracellular isoform of matrix metalloproteinase-2 impairs contractility of mouse myocardium. *Front Physiol*. 2014; 5:363. [PubMed: 25309453]
 32. Lovett DH, Mahimkar R, Raffai RL, Cape L, Zhu BQ, Jin ZQ, Baker AJ, Karliner JS. N-terminal truncated intracellular matrix metalloproteinase-2 induces cardiomyocyte hypertrophy, inflammation and systolic heart failure. *PLoS One*. 2013; 8(7):e68154. [PubMed: 23874529]
 33. Sun W, Liu DB, Li WW, Zhang LL, Long GX, Wang JF, Mei Q, Hu GQ. Interleukin-6 promotes the migration and invasion of nasopharyngeal carcinoma cell lines and upregulates the expression of MMP-2 and MMP-9. *Int J Oncol*. 2014 May; 44(5):1551–1560. [PubMed: 24603891]
 34. Zhou X, Ren Y, Liu A, Han L, Zhang K, Li S, Li P, Li P, Kang C, Wang X, Zhang L. STAT3 inhibitor WP1066 attenuates miRNA-21 to suppress human oral squamous cell carcinoma growth in vitro and in vivo. *Oncol Rep*. 2014 May; 31(5):2173–2180. [PubMed: 24676554]

35. Mukherjee R, Mingoia JT, Bruce JA, Austin JS, Stroud RE, Escobar GP, McClister DM Jr, Allen CM, Alfonso-Jaume MA, Fini ME, Lovett DH, Spinale FG. Selective spatiotemporal induction of matrix metalloproteinase-2 and matrix metalloproteinase-9 transcription after myocardial infarction. *Am J Physiol Heart Circ Physiol*. 2006 Nov; 291(5):H2216–H2228. [PubMed: 16766634]
36. Spinale FG, Janicki JS, Zile MR. Membrane-associated matrix proteolysis and heart failure. *Circ Res*. 2013 Jan 4; 112(1):195–208. [PubMed: 23287455]
37. Clark IM, Swingler TE, Sampieri CL, Edwards DR. The regulation of matrix metalloproteinases and their inhibitors. *Int J Biochem Cell Biol*. 2008; 40(6–7):1362–1378. [PubMed: 18258475]
38. Alfonso-Jaume MA, Mahimkar R, Lovett DH. Co-operative interactions between NFAT (nuclear factor of activated T cells) c1 and the zinc finger transcription factors Sp1/Sp3 and Egr-1 regulate MT1-MMP (membrane type 1 matrix metalloproteinase) transcription by glomerular mesangial cells. *Biochem J*. 2004 Jun 15; 380(Pt 3):735–747. [PubMed: 14979875]
39. Hadler-Olsen E, Fadnes B, Sylte I, Uhlin-Hansen L, Winberg JO. Regulation of matrix metalloproteinase activity in health and disease. *FEBS J*. 2011 Jan; 278(1):28–45. [PubMed: 21087458]
40. Dutta P, Courties G, Wei Y, Leuschner F, Gorbato R, Robbins CS, Iwamoto Y, Thompson B, Carlson AL, Heidt T, Majumdar MD, Lasitschka F, Eitzrodt M, Waterman P, Waring MT, Chicoine AT, van der Laan AM, Niessen HW, Piek JJ, Rubin BB, Butany J, Stone JR, Katus HA, Murphy SA, Morrow DA, Sabatine MS, Vinegoni C, Moskowitz MA, Pittet MJ, Libby P, Lin CP, Swirski FK, Weissleder R, Nahrendorf M. Myocardial infarction accelerates atherosclerosis. *Nature*. 2012 Jul 19; 487(7407):325–329. [PubMed: 22763456]
41. Zhang Y, Da Silva JR, Reilly M, Billheimer JT, Rothblat GH, Rader DJ. Hepatic expression of scavenger receptor class B type I (SR-BI) is a positive regulator of macrophage reverse cholesterol transport in vivo. *J Clin Invest*. 2005 Oct; 115(10):2870–2874. [PubMed: 16200214]
42. Fontes JA, Rose NR, Cihakova D. The varying faces of IL-6: From cardiac protection to cardiac failure. *Cytokine*. 2015 Jan 31.

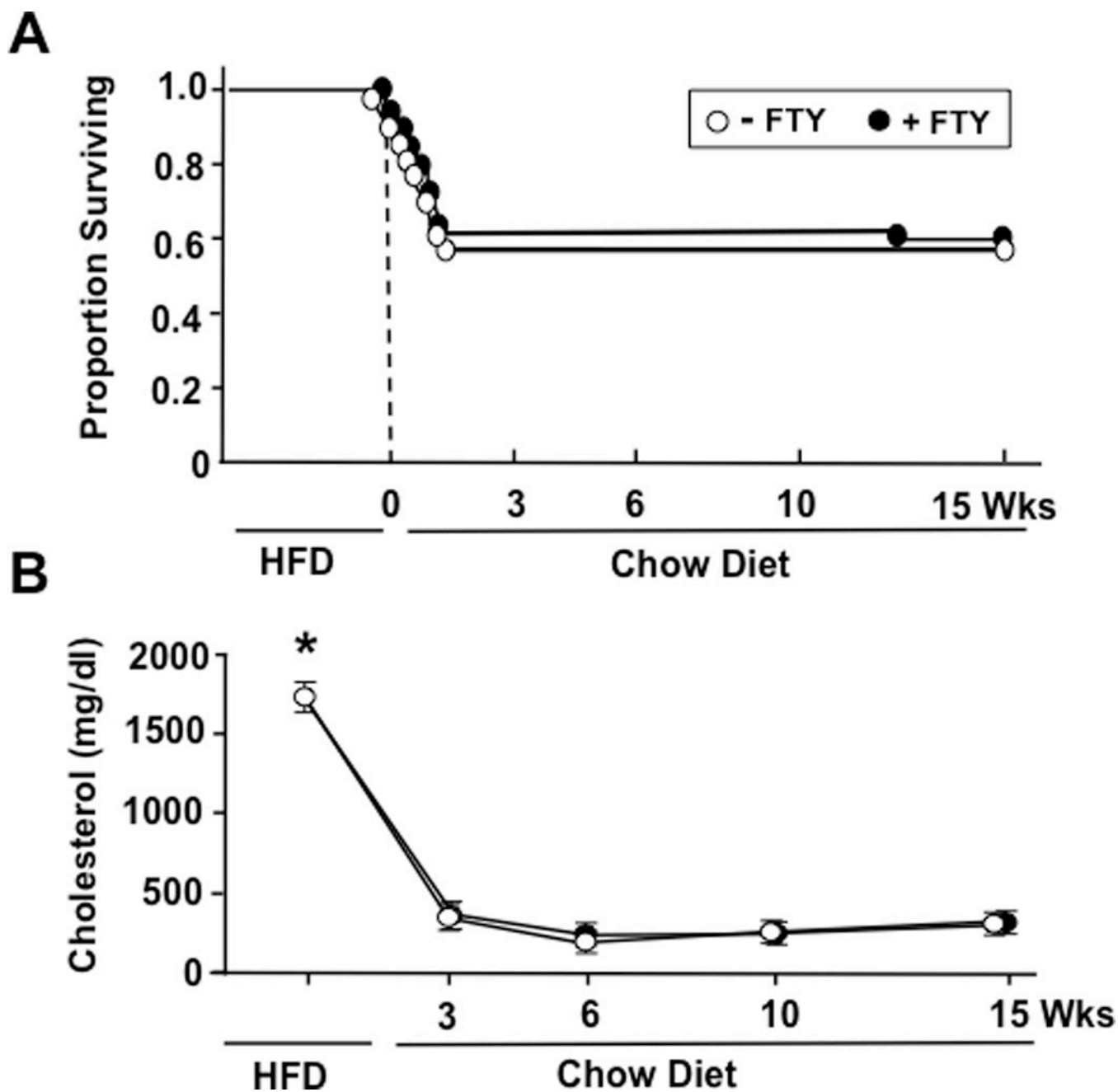
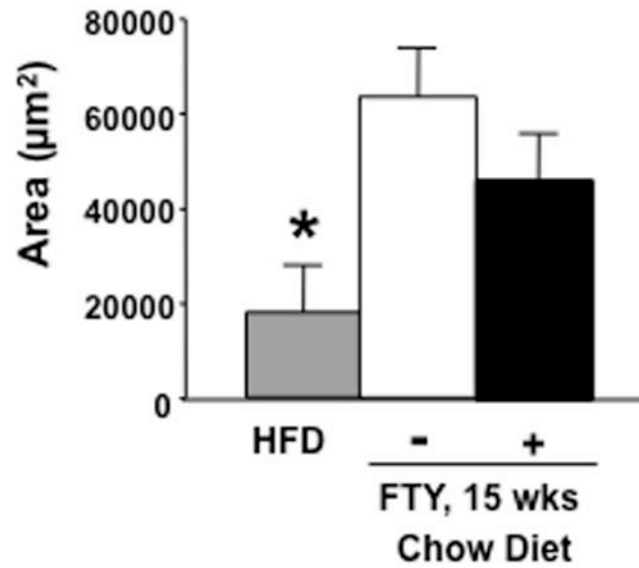
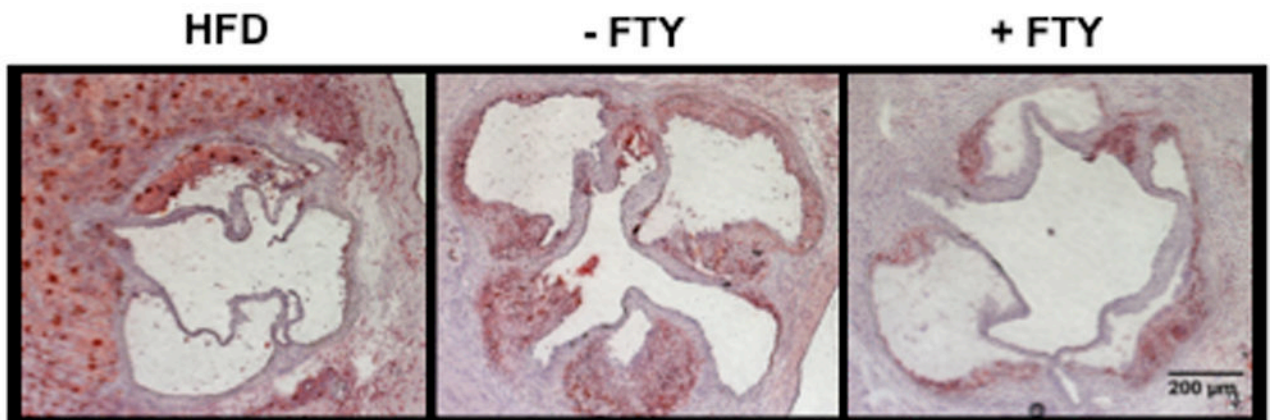


Figure 1.

A. Survival curves of *HypoE/SRBI*^{-/-} MX1-Cre mice (n=37–39) fed HFD followed by a chow diet with and without FTY720 for up to 15 weeks.

B. Plasma cholesterol levels (n=4–16) were measured after 3.5 weeks HFD (0) and at 3, 6, 10, and 15 weeks after start of FTY720 treatment.

Data are mean ± SEM. *P<0.05 versus control.

A**B****Figure 2.**

A. Quantification of aortic root lesion area from *HypoE/SRBI*^{-/-} MX1-Cre mice fed HFD for 3.5 weeks followed by 15 weeks chow diet with or without FTY720 (n=6-8). * $P < 0.05$ versus both + and - FTY720.

B. Representative images of aortic root lesions stained with ORO from *HypoE/SRBI*^{-/-} MX1-Cre mice fed HFD for 3.5 weeks followed by 15 weeks chow diet with or without FTY720.

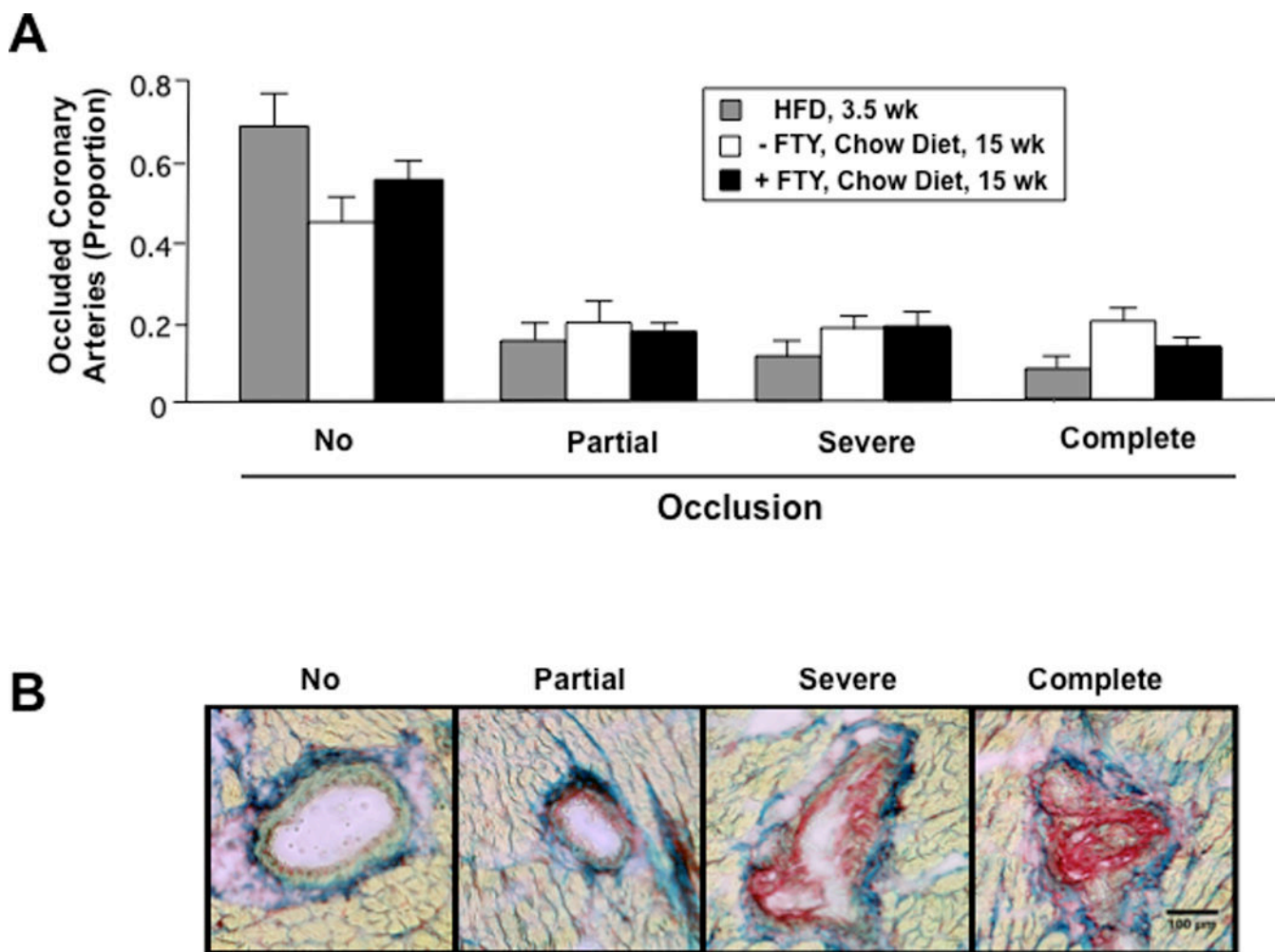


Figure 3.

A. Quantification of occluded coronary arteries from *HypoE/SRBI*^{-/-} MX1-Cre mice fed HFD for 3.5 weeks followed by 15 weeks chow diet with or without FTY720 (n=8–13). No, non-occluded (0–5%); Partial (5–50%); Severe (50–95%); Complete (100%).

B. Representative images of occluded coronary arteries stained with Picro Sirius Red and counterstained with Fast Green. No, non-occluded (0–5%); Partial (5–50%); Severe (50–95%); Complete (95–100%).

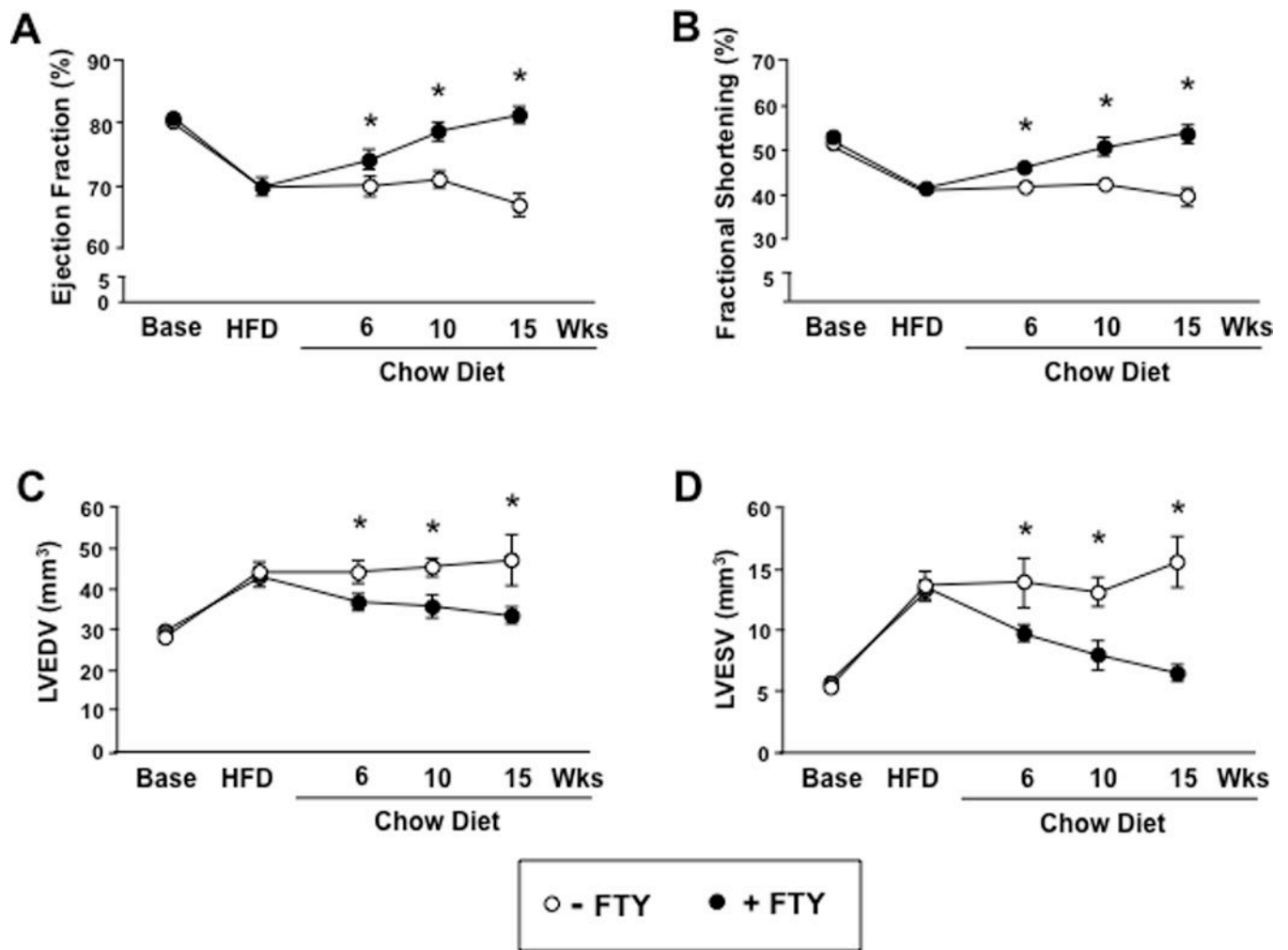


Figure 4. Echocardiographic measures of left ventricular performance (n=13–39). Ejection fraction (A) and fractional shortening (B), left ventricular end-diastolic volume (LVEDV) (C) and left ventricular end-systolic volume (LVESV) (D) in *HypoE/SRBI*^{-/-} MX1-Cre mice at baseline, fed a HFD for 3.5 weeks, or fed a chow diet with and without FTY720 for up to 15 weeks following HFD. Data are mean ± SEM. *P<0.05 (- FTY720 versus + FTY720).

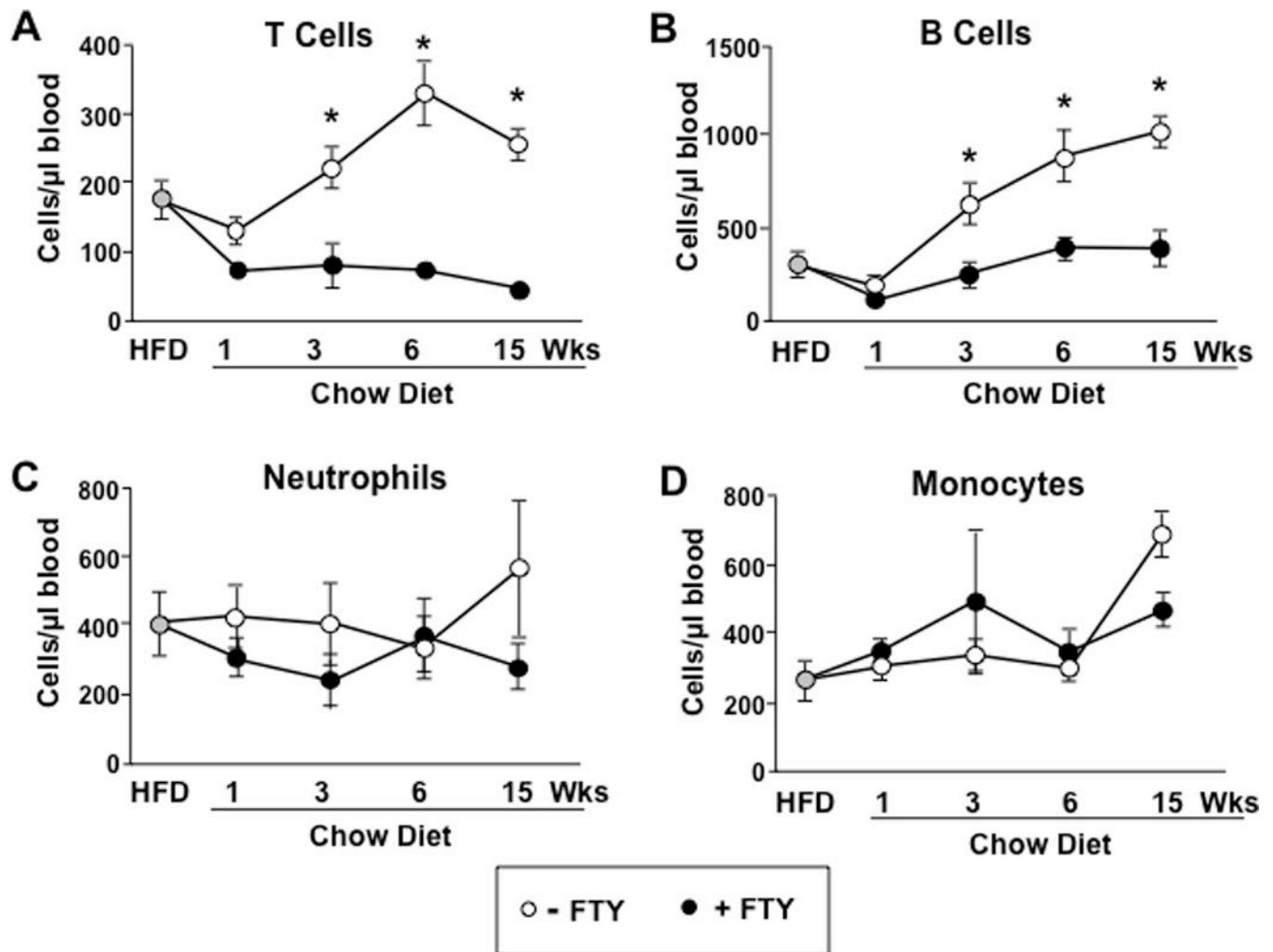


Figure 5.

Absolute numbers (n=5–13) of T cells (CD3⁺ B220⁻) (A), B cells (CD3⁻ B220⁺) (B), neutrophils (Ly6G⁺ CD11b⁺) (C) and monocytes (Ly6G⁻ CD11b⁺) (D) in peripheral blood in *HypoE/SRB1*^{-/-} MX1-Cre mice fed a HFD for 3.5 weeks and in mice at 1, 3, 6, and 15 weeks on a chow diet with or without FTY720 treatment. Data are mean \pm SEM. * P <0.05, - FTY720 versus + FTY720.

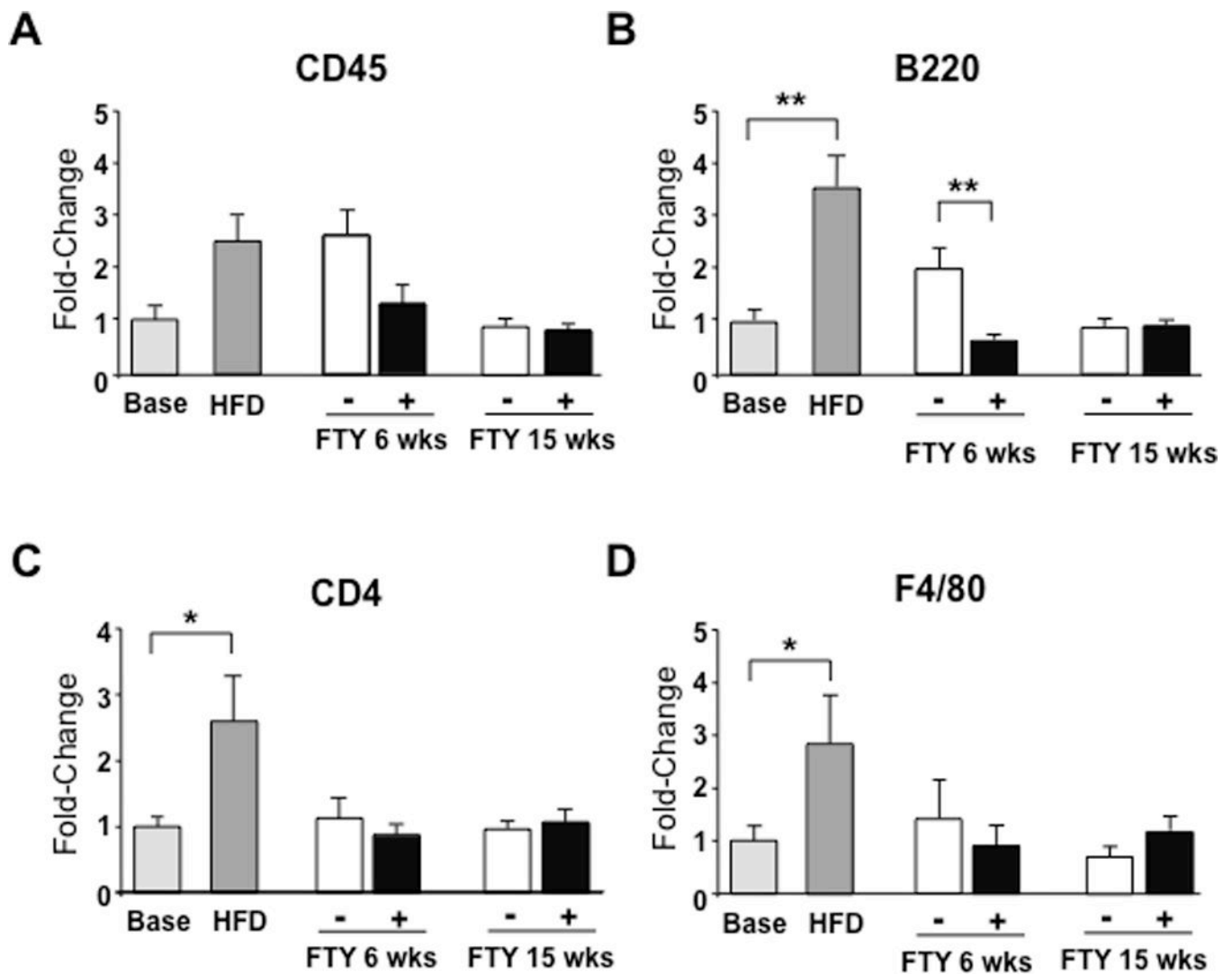


Figure 6. Relative mRNA expression levels (n=7) of CD45⁺ Leukocytes (A), B220⁺ B cells (B), CD4⁺ T cells, and F4/80⁺ macrophages in hearts from mice before HFD, immediately after HFD, and at 6 and 15 weeks post-HFD with or without FTY720. The relative quantity of mRNA was compared to baseline (Base, before HFD). Data are mean \pm SEM. * P <0.05, ** P <0.01

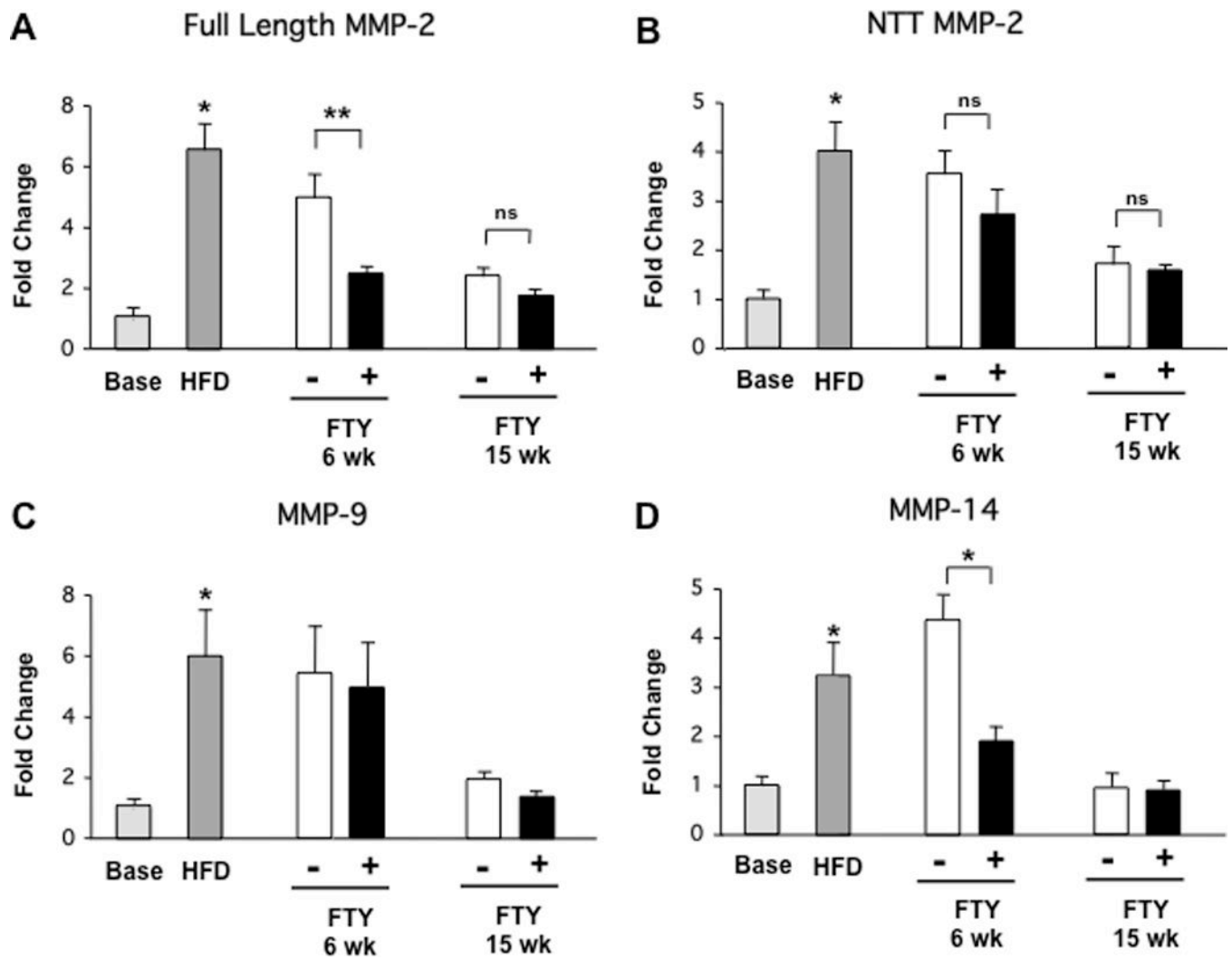


Figure 7. Relative mRNA expression levels (n=7) of full length (A), truncated (B) MMP-2, (C) MMP-9, and (D) MMP-14 in hearts from mice at baseline (base), immediately after high-fat diet (HFD), and 6 and 15 weeks post-HFD on a chow diet with or without FTY720. Relative mRNA expression was compared to baseline (Base, before HFD). Data are mean \pm SEM. * P <0.05

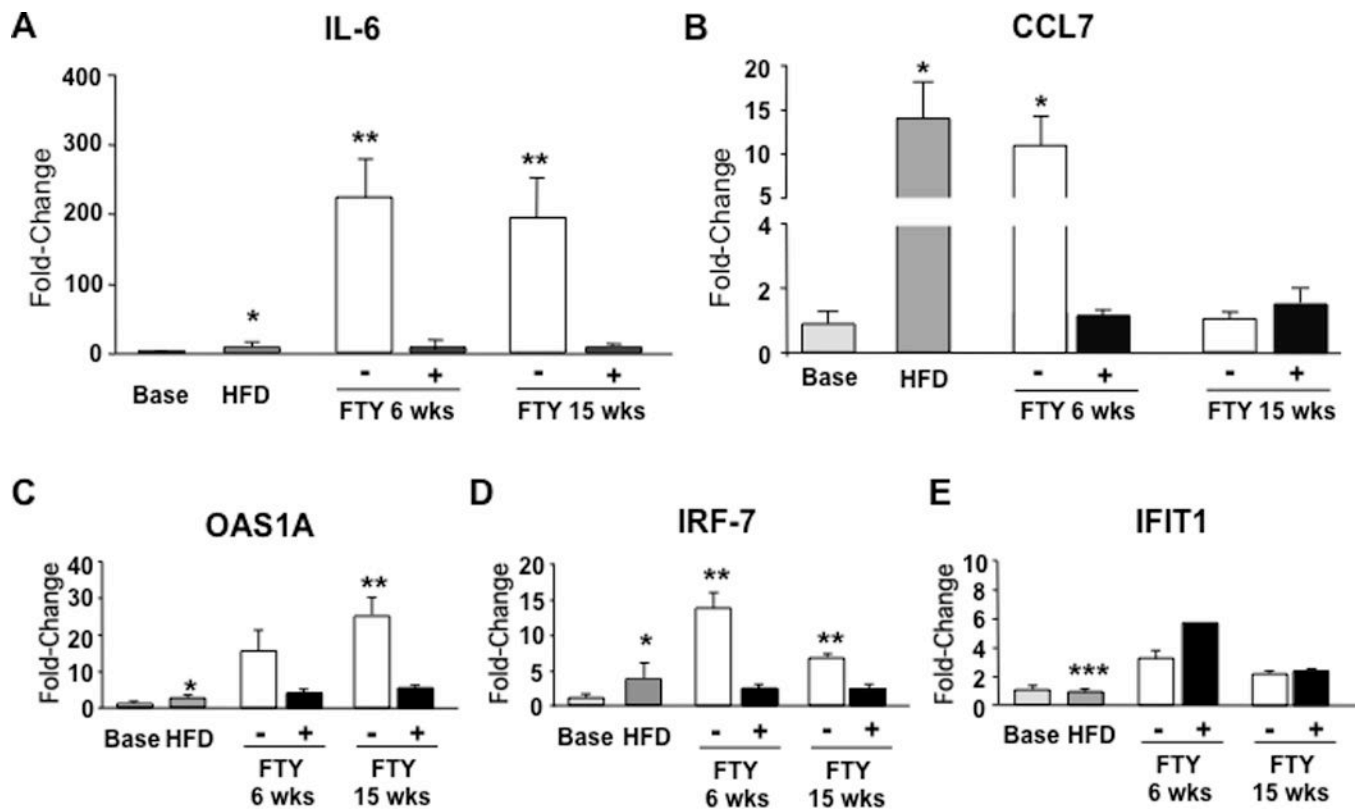


Figure 8. Relative mRNA expression levels (n=7) of IL-6 (A), CCL7 (B), OAS1A (C), IRF-7 (D), and IFIT1 (E) in hearts from mice before HFD, immediately after HFD, and at 6 and 15 weeks post-HFD with or without FTY720. The relative quantity of mRNA was compared to baseline (Base). Data are mean \pm SEM. * P <0.05, ** P <0.01

Table 1

TaqMan® Assay ID

Gene Name	Assay ID
CD45	Mm01293577_m1
CD4	Mm00000442754_m1
B220	Mm01293575_m1
F4/80	Mm00802529_m1
CCL7	Mm00443113_m1
GAPDH	Mm99999915_g1

Author Manuscript

Author Manuscript

Author Manuscript

Author Manuscript

Table 2

SYBR Green I primer sequence

Gene	Forward (5'→3')	Reverse (3'→5')
Full-length MMP-2	GACCTCTGCGGGTTCTCTGC	TTGCAACTCTCCTTGGGGCAGC
NTT MMP-2	GGCTCTGGAGCATGACCGCTT	TTGCAACTCTCCTTGGGGCAGC
2'-5' Oligoadenylate synthetase 1A (OAS1A)	ATTACCTCCTCCCGACACC	CAAACCTCCACCTCCTGATGC
Interferon-induced protein with tetratricopeptide repeats 1 (IFIT1)	TGTTGAAGCAGAAGCACACA	TCTACGCGATGTTTCCTACG
Interferon regulatory factor 7 (IRF-7)	CAGCGAGTGCTGTTTGGAGAC	AAGTTCGTACACCTTATGCGG
Interleukin 6 (IL-6)	GGGAAATCGTGAAATGAGAAA	AAGTGCATCATCGTTGTTACATA
β -2-microglobulin	TAAGCATGCCAGTATGGCCG	AGAAGTAGCCACAGGGTTGG

Author Manuscript

Author Manuscript

Author Manuscript

Author Manuscript